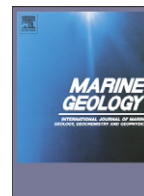




Contents lists available at ScienceDirect

Marine Geology

journal homepage: www.elsevier.com/locate/margeo

Evaluation of gas hydrate deposits in an active seep area using marine controlled source electromagnetics: Results from Opouawe Bank, Hikurangi Margin, New Zealand

Katrin Schwalenberg^{a,*}, Matthias Haeckel^b, Jeffrey Poort^{c,1}, Marion Jegen^b

^a Federal Institute for Geosciences and Natural Resources, Stilleweg 2, 30655 Hannover, Germany

^b IFM-GEOMAR, Wischhofstr. 1–3, 24148 Kiel, Germany

^c Renard Centre of Marine Geology, Ghent University, Krijgslaan 281 S8, 9000 Ghent, Belgium

ARTICLE INFO

Article history:

Received 30 October 2008

Received in revised form 13 May 2009

Accepted 9 July 2009

Available online xxx

Communicated by G.J. de Lange

Keywords:

marine CSEM

gas hydrate

methane seeps

Hikurangi Margin

New Zealand

ABSTRACT

Several known gas seep sites along the Hikurangi Margin off the east coast of New Zealand were surveyed by marine controlled source electromagnetic (CSEM) experiments. A bottom-towed electric dipole–dipole system was used to reveal the occurrence of gas hydrate and methane related to the seeps. The experiments were part of the international multidisciplinary research program “New Vents” carried out on German *R/V Sonne* in 2007 (cruise SO191) to study key parameters controlling the release and transformation of methane from marine cold vents and shallow gas hydrate deposits. Two CSEM lines have been surveyed over known seep sites on Opouawe Bank in the Wairarapa region off the SE corner of the North Island. The data have been inverted to sub-seafloor apparent resistivity profiles and one-dimensional layered models. Clearly anomalous resistivities are coincident with the location of two gas seep sites, North Tower and South Tower on Opouawe Bank. A layer of concentrated gas hydrate within the uppermost 100 m below the seafloor is likely to cause the anomalous resistivities, but free gas and thick carbonate crusts may also play a role. Seismic data show evidence of fault related venting which may also indicate the distribution of gas hydrates and/or authigenic carbonate. Geochemical profiles indicate an increase of methane flux and the formation of gas hydrate in the shallow sediment section around the seep sites. Takahe is another seep site in the area where active venting, higher heat flow, shallow gas hydrate recovered from cores, and seismic fault planes, but only moderately elevated resistivities have been observed. The reasons could be a) the gas hydrate concentration is too low, even though methane venting is evident, b) strong temporal or spatial variation of the seep activity, and c) the thermal anomaly indicates rather temperature driven fluid expulsion that hampers the formation of gas hydrate beneath the vent.

© 2009 Elsevier B.V. All rights reserved.

1. Introduction

Methane seepage from the seafloor in New Zealand has been first reported by Lewis and Marshall (1996). More seep sites have been found by New Zealand scientists during several cruises on *R/V Tangaroa*, and are described in e.g. Pecher et al. (2004) and Faure et al. (2006). However, the most extensive and complete investigations to date took place during *R/V Sonne* cruise SO191 in January–March 2007 within the “New Vents” project (Bialas et al., 2007, and this issue). The project “New Vents” focused on studying key parameters that control the release and transformation of methane from marine gas seep sites and shallow gas hydrate deposits on the Hikurangi Margin, an accretional convergent margin setting along the NE coast

of New Zealand. The aim of the controlled source electromagnetic (CSEM) experiment was to map the electrical nature of gas and gas hydrate filled sediments that are associated with the seeps. Both gas hydrate and gas are electrically insulating and enhance the electrical bulk resistivity in areas where they form in sufficient quantities. Methane, released from the seafloor through the dissociation of gas hydrate, or transported through the gas hydrate stability zone (GHSZ) along faults and fissures or in solution with the pore water, is believed to play a significant role in the global methane cycle. Gas seeps are known as areas of focused methane supply, and are often indicated by bubbles and flares ascending through the water column above the seep. Seep structures are often controlled by faults which can be imaged by seismic reflection data. Heat flow data identify areas of fluid advection characteristic of vent structures and fluid seepage. Geochemical profiles reveal methane flux through the shallow sediment section. Even though all these features have been observed in a variety of submarine settings worldwide, the process of fluid venting is not completely understood. In particular, what triggers gas venting, controls its volume, and sets the temporal variability?

* Corresponding author.

E-mail address: k.schwalenberg@bgr.de (K. Schwalenberg).

¹ Present address: Laboratoire de Géosciences Marines, Institut de Physique du Globe de Paris, 4, Place Jussieu, 7505 Paris, France.

Another open question is the amount and distribution of gas hydrate which has accumulated beneath these seeps. These hydrate accumulations may also be an important sink for the methane supply released from the seafloor. Within the “New Vents” project these objectives have been addressed with various geophysical, geochemical, and observational exploration methods. CSEM data, in this context, are sensitive to the presence and amount of gas hydrate. In principle, they cover the depth range of the entire gas hydrate stability zone while most other observations are confined to the seafloor or the shallow sediment section. Seismic data which cover the same depth range can be scattered or blanked by the presence of gas or hydrate. Thus CSEM data provide an important complement to the pool of sub-seafloor imaging tools.

Edwards (1997) showed that CSEM could be used for submarine gas hydrate investigation. The first prominent case study is known from the Northern Cascadia Margin offshore Vancouver Island. Yuan and Edwards (2000) reported on early marine CSEM field trials over known bottom simulating reflectors (BSRs). Riedel et al. (2002) analyzed seismic data from a nearby target area and revealed a series of seismic blank zones interpreted as cold vents. They suggested that blanking is the effect of intense hydrate formation inside the blank zone. Piston coring also gave evidence of shallow gas hydrate within the largest of the blank zones known as Bullseye. Schwalenberg et al. (2005) collected CSEM data along a profile over the vents and intersecting Bullseye. The resistivities derived from the CSEM data are clearly anomalous over the vents pointing at volumes of massive gas hydrate. The Bullseye vent was later on drilled during the Integrated Ocean Drilling Program, IODP Leg 311 (Riedel et al., 2006). A 40 m thick massive gas hydrate cap as well as anomalously high resistivities in wire line and logging-while-drilling logs have been observed in the same depth range (Riedel et al., 2006) which also explains the CSEM results.

More case studies are available from Weitemeyer et al. (2006) who reported on a CSEM survey over gas hydrate deposits on Hydrate Ridge, offshore Oregon, and Ellis et al. (2008) who conducted a CSEM survey to study a mud volcano and gas hydrate in the Gulf of Mexico.

Within the “New Vents” project marine CSEM was employed for the first time off the coastlines of New Zealand. CSEM data have been collected along four profiles in three target areas. Two of these areas, Opouawe Bank off the Wairarapa and LM9 (see insert in Fig. 1), are characterized by gas seepage and active seafloor venting. Analysis of a CSEM transect across Porangahau Ridge is subject of Schwalenberg et al. (in review). In this paper we present results from two CSEM lines surveyed on Opouawe Bank in the Wairarapa region (Fig. 1). Our models show highly elevated resistivities beneath the gas seeps. The most plausible explanation is that large amounts of gas hydrate have accumulated below the seep sites. We apply Archie's Law (Archie, 1942) to estimate the gas hydrate concentration associated with the anomalous resistivity at one seep site. In the discussion we also include results from seismic, heat flow, and geochemical observations from the same target area.

2. Study area

The Wairarapa region is part of the Southern Central Hikurangi Margin off the east coast of New Zealand's North Island, an active convergent margin system formed by the westward oblique subduction of the Pacific plate beneath the Australian plate. In its central part the Hikurangi Plateau, an elevated 10–15 km thick oceanic crust (Davy and Wood, 1994), is subducted beneath the Australian plate at slow rates (about 40–50 mm/yr) and low angle (about 3°) (Barnes et al., 2009—this issue). The central margin off the Wairarapa is dominated by accretionary tectonics and a classical imbricated frontal wedge which is poorly drained and over-pressured. According to Townend

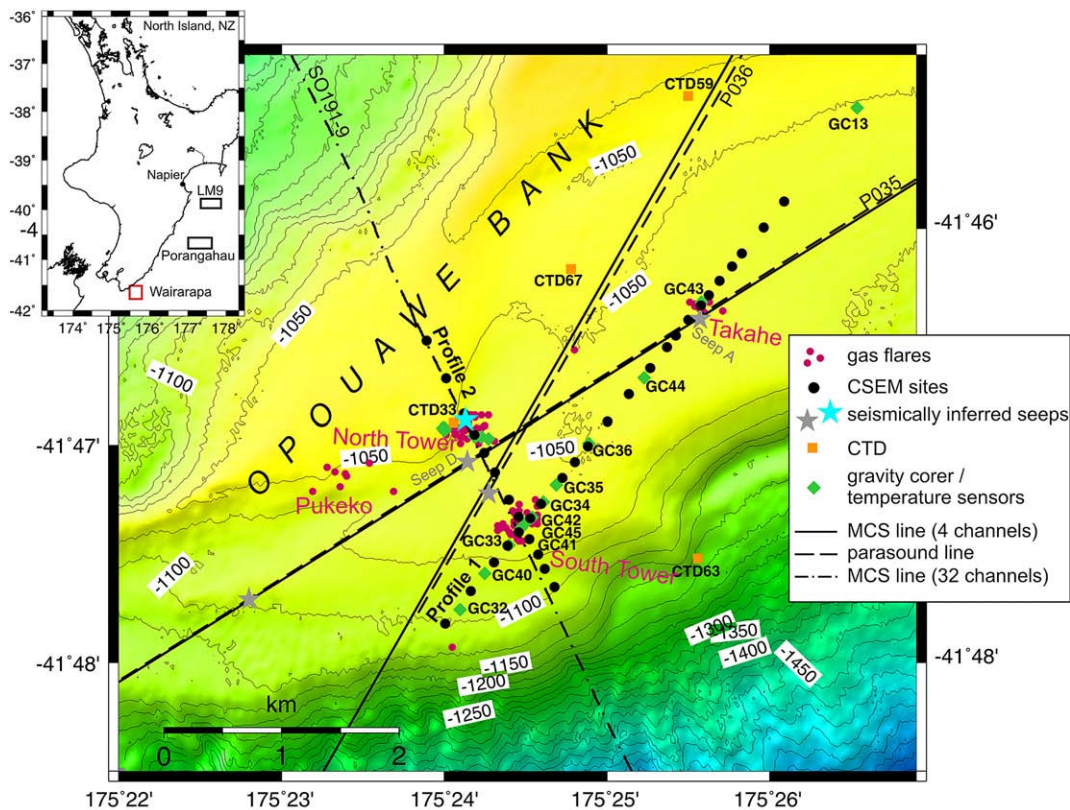


Fig. 1. Bathymetric map of Opouawe Bank in the Wairarapa target area showing seep sites and geophysical observation sites as indicated in the legend. The insert map also shows two other target areas where CSEM data were collected. Grey stars mark seismically inferred seep sites by Netzeband et al. (2009—this issue), the blue star refers to a seep site described in Barnes et al. (2009—this issue). (For interpretation of the references to colour in this figure legend, the reader is referred to the web version of this article.)

(1997) and Barnes et al. (2009–this issue) there is plenty of fluid flow within the Hikurangi Margin which promotes the observed widespread gas seep sites and associated chemosynthetic fauna as well as the formation of gas hydrate.

Widespread BSRs have been observed along the margin (e.g. Katz, 1982; Lewis and Marshall, 1996; Henrys et al., 2003) indicating the presence of gas hydrate at the base of the gas hydrate stability zone and free gas below. After the first comprehensive description of gas seep sites around New Zealand by Lewis and Marshall (1996), research has been intensified to study the nature of these seeps, the origin of the gas supply, the link to sub-seafloor gas hydrate formation, and the overall integration in the tectonic subduction setting. Interestingly, all known seep sites found on the Hikurangi Margin are located on the crests of thrust fault ridges indicating a clear relationship between seeps and major faults (Barnes et al., 2009–this issue). On Opuawe Bank, methane seepage was first discovered in echo sounder data and video observations by New Zealand scientists on R/V *Tangaroa*, particularly cruise TAN0616. The first detailed investigation of this target area took place on R/V *Sonne* cruise SO191 within the “New Vents” project (Bialas et al., 2007).

Fig. 1 shows a map of the Wairarapa survey area. Opuawe Bank, a NE–SW striking plateau in water depth of 1000–1100 m, is one of the characteristic ridge and basin systems of the accretionary wedge. Several active seep sites called North Tower, South Tower, Pukeko, Takahe, and Tui have been identified (Greiner et al., in review). These seep sites were first detected as areas of individual gas flares in hydro-acoustic data and video observations (Klaucke et al., 2009–this issue; Bialas et al., 2007). A BSR which is interrupted between the seismically identified seep sites has been observed around 600 m below the seafloor (mbsf) along profiles P035, P036, and SO191-9 (Figs. 3 and 4 in Netzeband et al. 2009–this issue and Fig. 8 in Barnes et al., 2009–this issue). The two CSEM lines are crossing South Tower and Takahe (Profile 1), and North Tower and South Tower (Profile 2). For comparison the locations of some other experiments which have been conducted during the SO191 expedition are also marked on the map.

3. Marine CSEM

Marine CSEM is based on the diffusive propagation of electromagnetic (EM) signals emitted from a source dipole (Tx) on or close to the seafloor. The EM signal travels away from the source dipole through the conductive seawater where it is attenuated quickly, and through the more resistive seafloor sediments. It is recorded by one or more receivers located on the seafloor at some distance away from the Tx. The part of the signal passing through the seafloor arrives at the receivers first. Cheesman et al. (1987) derived the theoretical background for various magnetic and electric seafloor dipole–dipole configurations. We look at the signals in the time domain. Here, arrival times as well as amplitudes and shapes of the signals recorded at the receivers over a time range clearly depend on sub-seafloor resistivity structure (e.g. Edwards, 1997). The presence of resistive materials, like gas hydrate and gas, enhances the electric field and thus the observed resistivity.

3.1. Electrical resistivity

The physical parameter derived from CSEM data is the electrical resistivity ρ , or its reciprocal, the electrical conductivity σ . For marine sediments the electrical conductivity is foremost a function of the porosity, the type of the pore fluid which is typically seawater, and the connectivity of the pore fluid. The sediment grain matrix itself is generally non-conductive. The conductivity of seawater mainly depends on temperature and salinity and is typically in the order of $\sigma = 3.0$ – 3.5 S/m on the seafloor which corresponds to $\rho = 0.286$ – 0.33 Ω m. The physical properties of seawater can be measured with e.g. a conductiv-

ity–temperature–depth (CTD) device. CTD data on Opuawe Bank revealed sea-bottom conductivities of 3.3 S/m. Typical resistivity values for the shallow seafloor sediment section are between 0.8 and 1.5 Ω m.

Gas hydrate itself is electrically insulating. The distribution of gas hydrate within the stability zone is manifold. Gas hydrate has been observed as pore infill, along grain contacts, filling fissures and cracks, or replacing parts on a centimeter to meter scale of the entire sediment volume. In all cases the observed resistivity is elevated where hydrate forms in sufficient quantities. A simple approach to estimate the average gas hydrate concentration from resistivity data is given by Archie's (1942) empirical porosity–resistivity relation for a two-phase porous system consisting of sediment grains and seawater:

$$\rho_f = a\rho_w\phi^{-m}, \quad (1)$$

where ρ_f is the measured formation resistivity, ρ_w is the resistivity of seawater, ϕ is the sediment porosity, a is a constant, and m the cementation factor. If a third phase is present, i.e. gas hydrate, this relation can be generalized to

$$\rho_f = a\rho_w S_w^n \phi^{-m}, \quad (2)$$

where S_w is the pore water saturation factor, n is the saturation coefficient which is often equal to m , and $S_h = (1 - S_w)$ is accordingly the fractional gas hydrate concentration.

In Fig. 2 we show curves of Archie's resistivity–porosity–relation for different settings of m which typically increases with sediment depth as the grains become less spherical (Evans et al., 1999). Jackson et al. (1978) found cementation factors m between 1.4 and 2 for various natural and artificial marine sediment samples. This is displayed by the solid purple curve in Fig. 2. Based on these results an observed formation resistivity of 1 Ω m corresponds to an average porosity of about 50%. An increase in resistivity to 3 Ω m corresponds to a porosity of 23%, and a bulk resistivity of 5 Ω m results in a bulk porosity of below 16%. This clearly demonstrates that resistivity is a robust parameter to identify areas of significant porosity reduction, e.g. due to the replacement of pore fluids with resistive matters like gas hydrate.

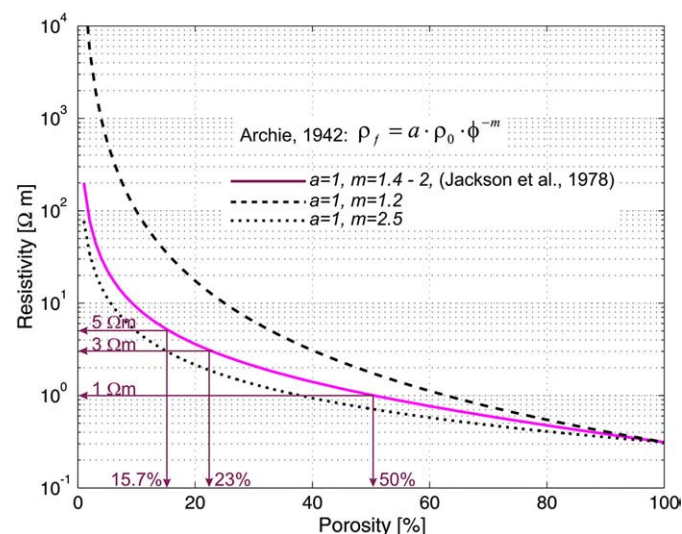


Fig. 2. Archie's (1942) empirical resistivity porosity relation for a two-phase porous system (modified from Evans et al., 1999). Seawater resistivity is set to 0.3 Ω m. The cementation factor m depends on the shape of the grain particles and increases with sediment depth where the grains become less spherical. Applying Jackson's set of Archie parameters an observed formation resistivity of 1 Ω m corresponds to an average porosity of 50%. An increase in resistivity to 3 Ω m corresponds to a porosity of 23%, and a bulk resistivity of 5 Ω m results in a bulk porosity of below 16%.

Archie's relation breaks down when the gas hydrate forms in solid layers or is not confined to the pore structure. However, the size of the average sediment volume surveyed by our CSEM system is in the scale of a meter to some hundred meters. We therefore assume that Archie's Law can be applied to estimate the average hydrate concentration from CSEM data, and the method can be used to derive the potential hydrate volume at the South Tower seep site.

3.2. Instrumentation

A unique bottom-towed electric dipole–dipole system, designed and built at the University of Toronto, was used to study the gas seep sites and gas hydrate on the Hikurangi Margin. On the seafloor, the system consists of a transmitting dipole (Tx) with a dipole moment of $5 \text{ A} \times 124 \text{ m}$ and two receiving dipoles (Rx1, Rx2) which are towed behind the Tx at distances of 172 m (to Rx1) and 275 m (to Rx2) (Fig. 3). The complete seafloor system has a total length of ~360 m. A heavy weight called the pig is attached to the front of the array to keep it on the seafloor. The seafloor array is connected to the coaxial oceanographic cable and is towed at some distance behind the ship. The signal source is located on the ship. The current signal is sent down to the Tx via the coaxial cable. We used a square wave signal with a period of 3.36 s and bidirectional amplitude of $\pm 5 \text{ A}$ which was limited by the gauge of the coaxial cable.

An Ag/AgCl electrode is mounted at either end of the 15 m long receiving dipoles. Each receiving dipole is equipped with a self-contained, battery powered electronic unit which digitizes and records the voltage between the electrodes at a sampling rate of close to 1 ms. The electronic parts and battery packs are inside a pressure cylinder attached to the front end of the Rx.

A third identical electronic unit stays onboard during the experiment and records the transmitted signal during the deployment in synchronization with the two seafloor receiver units. For instrument positioning an acoustic transponder was attached to the pig. The array is towed on the seafloor along profiles. However, to get clean data it is necessary to stop the array at a series of sites. Data recorded during transits between the sites are noisy and cannot be used for the analysis.

A minimum separation of 150 m between sites was achieved over the seeps while the average distance was 250 m away from the seeps. The data show the largest response to structures located between transmitting and receiving dipoles down to a sediment depth of approximately half the distance between Tx and Rx (Edwards, 1997).

3.3. Data analysis

Pseudo-continuous periodic time series of the ambient electric field have been collected for about 15 min at each measurement site. A stacked data set has been derived for both receivers at each site. Fig. 4 shows stacked data sets recorded with Rx2 for all sites along Profile 1. Sites 3–7 are located at South Tower and differ clearly from the rest of the profile. The amplitudes are higher and the signal arrives at earlier times. Both effects suggest that resistive material is present at depth below the seafloor.

The data collected at the receivers result from the convolution of the earth impulse response with the source signal. The sub-seafloor resistivity can be found by one-dimensional (1D) inversion. We used a program provided by C. Scholl (University of Toronto, 2007, unpublished software) to calculate apparent resistivity profiles and 1D layered models. Inputs in the program are the source function, stacked receiver data sets, and errors. The program also requires a starting model which can be either a uniform or horizontally layered halfspace. Water depth and seawater conductivity are preset. Marquardt inversion has been applied to calculate apparent resistivities, and Occam inversion to find a layered model solution. However, inversion is a non-unique process and the models presented in the following section have been chosen out of number of inversion results based on data fit and plausibility.

4. Results

4.1. CSEM Profile 1

Fig. 5a shows the apparent resistivities along Profile 1. The CSEM data sets from both receivers have been inverted separately (blue

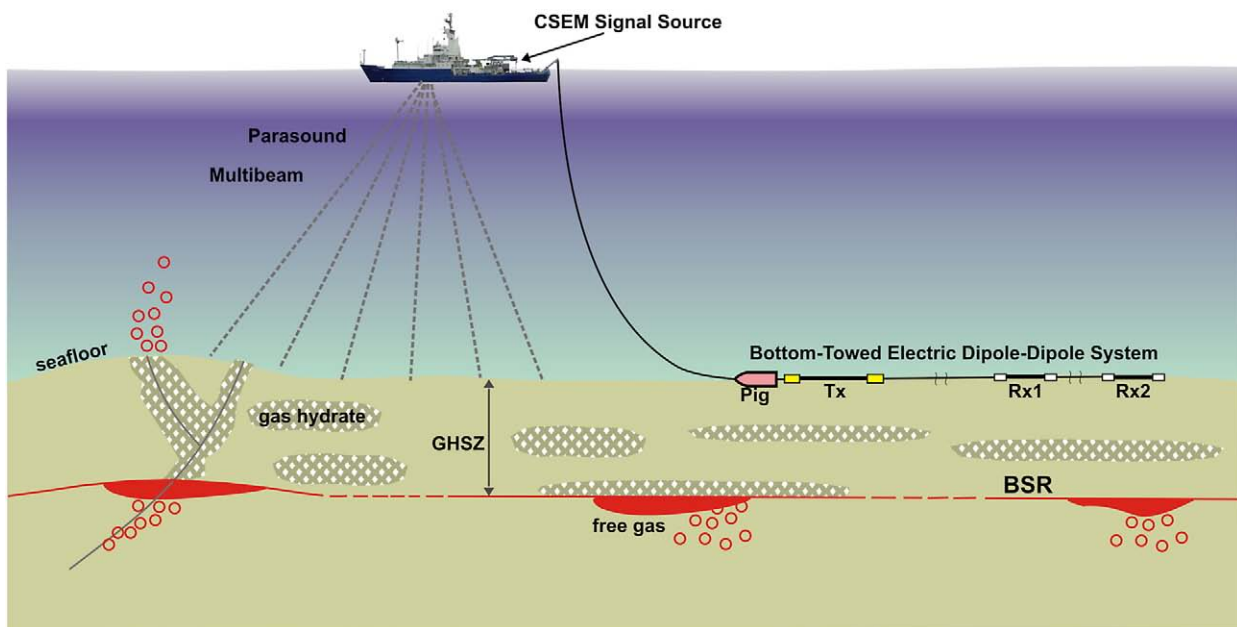


Fig. 3. Set-up of the inline electric dipole–dipole system. Two receiving dipoles Rx1 and Rx2 (15 m each) are towed on the seafloor behind a transmitting dipole Tx (126 m) at distances of 172 m (Rx1) and 275 m (Rx2). The source signal, a square wave of $\pm 5 \text{ A}$ amplitude and period of 3.36 s, is generated by a current transmitter on the ship and is sent down to the Tx dipole via the coaxial cable. The electromagnetic disturbance propagates away from the Tx through the seawater and the sediments and is recorded at the receivers. Arrival time, signal shape, and amplitude depend on seafloor conductivity structure.

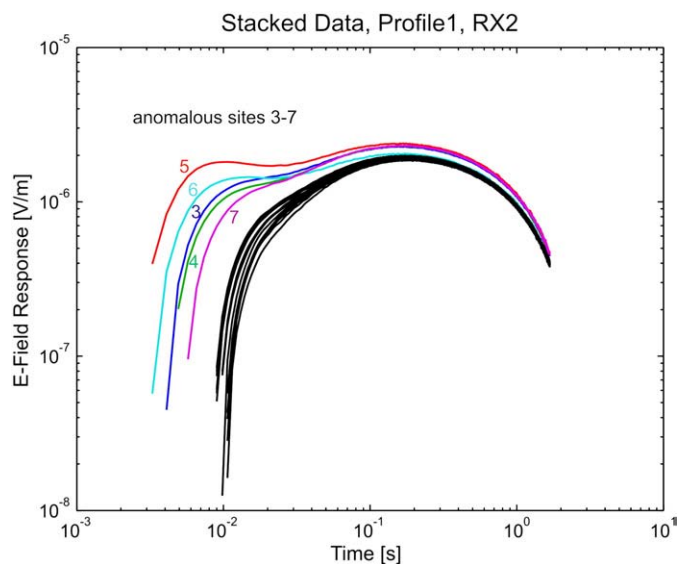


Fig. 4. Stacked data collected at Rx2 for all sites along Profile1 in a double logarithmic plot. Sites 3–7 are clearly anomalous and differ from the remaining sites, particularly in the early times.

curve: Rx1, red curve: Rx2, and jointly (black curve). The most remarkable result is the pronounced anomaly observed over the gas seeps at South Tower. The apparent resistivities are as high as $10 \Omega\text{m}$ while the rest of the profile shows normal values between 1.1 – $1.5 \Omega\text{m}$. The anomaly at South Tower is much smaller when only data from Rx1 have been used while the apparent resistivity profile derived from data of Rx2 is similar to the profile obtained from joint inversion. This suggests that the observed anomaly at South Tower is caused by resistive materials, i.e. gas hydrate, at intermediate depths below the seafloor which have a larger influence on the data collected at Rx2.

Around the Takaha seep site, apparent resistivities derived from both the joint inversion and the single inversion of data from Rx2 are

slightly elevated in comparison to the rest of the profile outside the seeps.

The vertical structure at each site was derived by joint inversion of data from Rx1 and Rx2 to a 1D layered model. In Fig. 5b the individual models are stitched together for a 2-D presentation. The models show a layer of very conductive and probably highly porous sediments close to the seafloor. Below South Tower the inversion reveals a thick layer of highly anomalous resistivity above $3 \Omega\text{m}$ in the depth interval of ~ 40 – 80 mbsf. Some resistivities are locally even higher than $10 \Omega\text{m}$. Also at Takaha the resistivities are slightly elevated at depths below 40 mbsf. Here, the areas of anomalous resistivity are patchy and not as distinct as below South Tower. However, there is a clear correlation between gas seepage from the seafloor and elevated resistivities at intermediate depths below which we attribute to the presence of gas hydrate reservoirs. The very high conductivities below the resistive layer at South Tower are in the order of seawater or even more conductive. We have not fully understood yet what is causing these high conductivities. Possible explanations are a) those deeper parts of the models are not resolved by the data and the inverse algorithm may be generating unreasonable high conductivities, b) the resistivity distribution around the seep is rather 3D and the high conductivities may be artifacts of the 1D approach, c) calibration errors in the late time data, sensitive to the deeper part of the models, may result in lower electric fields and thus in higher electrical conductivities, or d) salt exclusion during hydrate formation may significantly increase the formation conductivity. However, it does not question the existence of the resistive layer which is clearly indicated by the apparent resistivities in Fig. 5a.

4.2. Gas hydrate concentration along Profile 1

Fig. 6 shows apparent porosities (black curve) derived from the apparent resistivity profile in Fig. 5a) setting Archie's parameters empirically to $a = 1$ and $m = 2$ (Eq. (1)). Experimental estimates for a and m based on core or logging data are not available for the survey area. However, apparent porosities derived with $m = 2$ are around

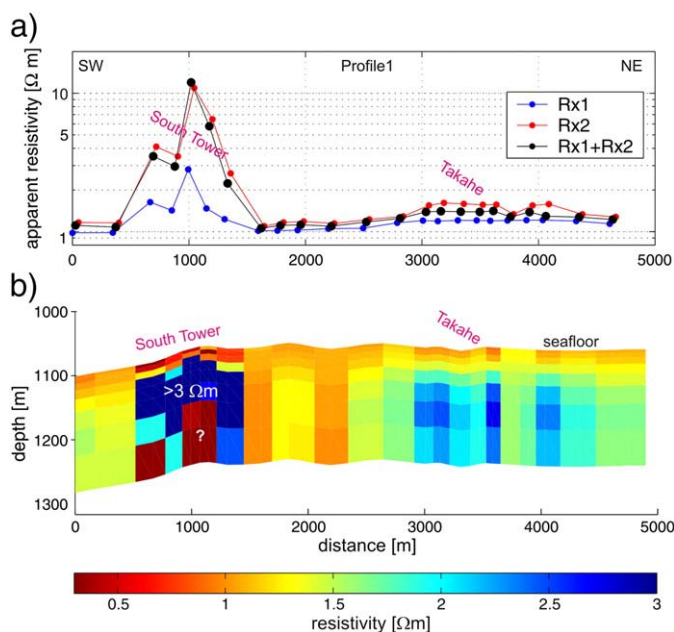


Fig. 5. a) Apparent resistivities derived along Profile 1. Data from Rx1 and Rx2 have been inverted separately (blue and red curves) and jointly (black curve). At South Tower the resistivities are extremely high. Apparent resistivities derived with Rx2 are much higher than with Rx1. This suggests that resistive materials, i.e. gas hydrate, exist at depth. At Takaha, apparent resistivities are only slightly above the background resistivity. b) Stitched section of joint 1D inversion results applying Occam inversion. Close to the seafloor the models show a layer of conductive sediments. Very anomalous resistivities ($>3 \Omega\text{m}$, locally $>10 \Omega\text{m}$) occur at depths of about 40 – 80 mbsf beneath South Tower. The high conductivities below the resistive layer at South Tower are yet not fully understood (see text). Around Takaha seep site the resistivities are also elevated in the same depth interval, but the distribution is patchy and the values are less anomalous. (For interpretation of the references to colour in this figure legend, the reader is referred to the web version of this article.)

50% for the sites away from the seeps which is in agreement with the shallow sediment porosities derived from gravity cores along Profile 1 (Fig. 8). At South Tower the apparent porosity is clearly reduced. There is a small porosity reduction around Takahe. We calculate the fractional gas hydrate concentration from Eq. (2) and derive the total volume percent by multiplication with the 50% background porosity (green curve in Fig. 6). Outside South Tower the gas hydrate concentration is close to zero. At South Tower we reveal considerable gas hydrate concentrations between 13 and 34% in an estimated depth interval of at least 50 m. Increasing or decreasing the cementation factor m to 1.8 or 2.2, respectively, enhances or reduces the gas hydrate concentration by around 2%. At Takahe the estimated hydrate concentration is only 2–3% above the background value. This does not rule out that localized gas hydrate and/or gas pockets exist below Takahe. Neither does our assessment rule out that more gas hydrate exists at deeper levels close to the BSR which is around 600 mbsf (Netzeband et al., 2009–this issue) where we have no or negligible data coverage with our chosen CSEM configuration.

4.3. CSEM Profile 2

Along CSEM Profile 2 only data from the second receiver (Rx2) are available. The apparent resistivity profile in Fig. 7a) shows generally high values and two anomalies which appear to be linked to the seep sites at North Tower and South Tower. A stitched section of 1D layered inversion results along Profile 2 is shown in Fig. 7b). Note that different colour bars are used in Figs. 5 and 7. In the uppermost 80 mbsf the resistivities are consistently above 2.5 Ωm with exception at the SE end of the profile. The results shown in this figure have to be interpreted carefully: The vertical resolution is limited because only data from one receiver are included. In particular, the conductive parts below 80–100 mbsf are yet not fully understood as described above. Nevertheless, the data fit is better for the 1D layered models (rms ~ 1) than for the apparent resistivities in Fig. 7a). We think the high resistivities obtained along Profile 2 indicate there are large amounts of gas hydrate below the seafloor. There is also reasonable agreement between the apparent resistivities close to where Profiles 1 and 2 intersect which supports the results along Profile 2.

5. Discussion

The resistivity anomalies observed on Opuawe Bank suggest that considerable volumes of gas hydrate have accumulated at depth below the seep sites at North Tower and South Tower, but there is a smaller amount at Takahe. Free gas, another candidate that would increase the measured bulk resistivity, is evidently present, at least in the very shallow seafloor section beneath the seeps. However, we don't think that free gas will make up for a large volume, at least not enough to produce the observed resistivity anomalies. Free gas will be likely confined to the fault planes, and to cracks and fissures. Under normal conditions we assume that methane will be transported upwards

through the sediment section in solution, and gas hydrate will be formed within the GHSZ from dissolved methane. Along deep reaching faults the fluid flow can be accordingly high, and free gas may be transported all the way up to the seafloor as observed by Netzeband et al. (2009–this issue).

Carbonates formed under anaerobic conditions on or close to the seafloor can be also very resistive. At the seep sites on Opuawe Bank they have been observed as widespread patches in geo-acoustic data (Klaucke et al., 2009–this issue) and in video observations (Bialas et al., 2007). Netzeband et al. (2009–this issue) observed high amplitude reflections in parasound and seismic data at two seep sites near North Tower and Takahe at depths of 25 mbsf and 10 mbsf, respectively, and discuss that these reflections can be attributed to either gas hydrates or carbonate crust. However, there is no further evidence that massive carbonates exist below the seep sites. Therefore it is questionable to which extent carbonates may account for the observed resistivity anomalies. We think that thick layers of carbonate crust, if present, may contribute, but do not entirely explain the observed resistivity anomalies.

Gas hydrate, in contrast, may form area-wide in large quantities. Massive layers of gas hydrate have been found in bore holes of a number of ocean drilling programs (e.g. on the Cascadia Margin offshore Vancouver Island (IODP 311, Riedel et al., 2006) and offshore India (NGHP 01, Collett et al., 2008).

On Opuawe Bank the CSEM results suggest that gas hydrate has formed in an intermediate layer below the seep sites. There is no indication that gas hydrate is present outside the seep areas, at least not within the first 100 mbsf. Here, the resistivities have normal background values between 1.1 and 1.3 Ωm . There might be a few volume percent (<3%) of gas hydrate, but the respective resistivity variations could be also caused by sediment heterogeneities. Gas hydrate may be also present at deeper parts closer to the BSR where our instrumental set-up provides little to no data coverage.

We derived an estimate of the gas hydrate volume that may have accumulated below South Tower. The gas hydrate concentrations shown in Fig. 6 are an average for the 3D area between transmitting and receiving dipoles down to a depth of about half the transmitter–receiver offset. Assuming a 50 m thick cylinder below each anomalous site with a 100 m diameter is therefore a conservative guess. We apply the gas hydrate concentrations derived at sites 3–7 (Fig. 6) to estimate the hydrate volume at each anomalous site which adds up to the total gas hydrate volume at South Tower. This results in a volume of $4.46 \times 10^5 \text{ m}^3$. Setting the cementation factor m in Eq. (2) to $m = 1.8$ and $m = 2.2$ results in $4.82 \times 10^5 \text{ m}^3$ and $4.07 \times 10^5 \text{ m}^3$, respectively, which differs by roughly 10% from our estimate. With a hydrate to free gas ratio of 1:182 STP (standard pressure and temperature conditions, i.e. $P = 1 \text{ bar}$, $T = 25 \text{ }^\circ\text{C}$, a density of gas hydrates of 0.9 g/cm^3 , and a stoichiometry of $\text{CH}_4 \times 5.9 \text{ H}_2\text{O}$) the according free gas volume is $8.12 \times 10^7 \text{ m}^3$.

There is further evidence of focused fluid flow and active venting at Opuawe Bank. A large number of seeps have been identified in seismic data by Netzeband et al. (2009–this issue) and Barnes et al. (2009–this

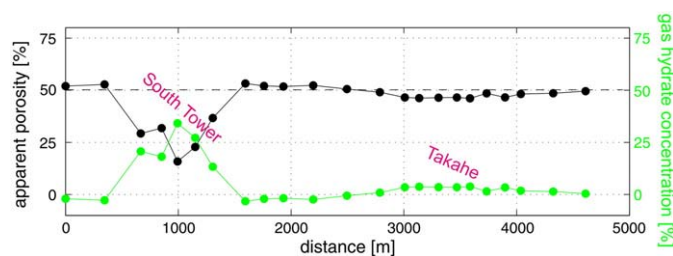


Fig. 6. The apparent porosity profile (black curve) has been derived from the apparent resistivity profile in Fig. 5a using Archie's Law with $a = 1$ and $m = 2$. At South Tower the average porosity is clearly reduced, at sites 5 and 6 even below 25%. Average baseline porosities are around 50% which is in agreement with porosity data from gravity cores. The estimated gas hydrate concentration (green curve) at South Tower is partly above 25% of the total sediment volume. At Takahe gas hydrate amounts to only 2–3%. (For interpretation of the references to colour in this figure legend, the reader is referred to the web version of this article.)

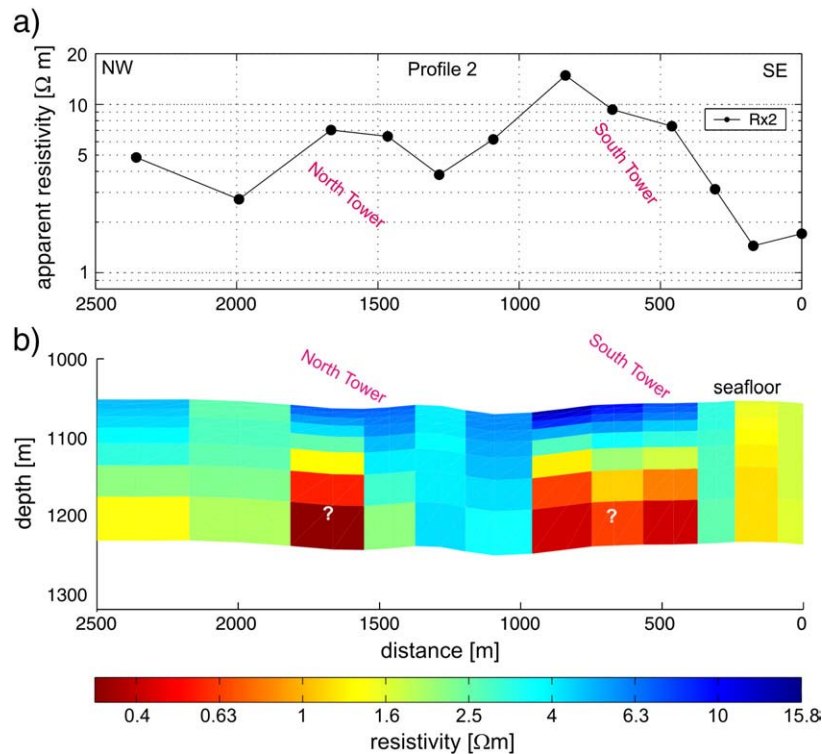


Fig. 7. a) Apparent resistivities along Profile 2. Only data from the second receiver are available for this transect. The resistivities are generally higher than along Profile 1. At North Tower and South Tower the values are locally even more elevated. b) The stitched section of 1D models shows a shallow, about 60 m thick resistant layer with more anomalous values below the seep sites. The data fit is much better for the 1D models than for the apparent resistivities (rms misfit = 1). The very high conductivities at depth are yet not fully understood (see text). Note: colour scale is logarithmic unlike in Fig. 5. (For interpretation of the references to colour in this figure legend, the reader is referred to the web version of this article.)

issue) using multi channel seismic (MCS) data. The seismic acquisition lines and the seafloor positions of these seeps are marked in Fig. 1 as gray and blue stars, respectively. Some of these seeps are within the gas seep areas, e.g. at North Tower and Takahe, but some of them are located outside. These seep structures are related to polygonal faults which pierce the BSR and are thought to be gas chimneys through the GHSZ to the seafloor (Netzeband et al., 2009-this issue).

5.1. Geochemical analysis

A four meter long gravity corer was used to collect core samples for geochemical analysis along CSEM Profile 1 (Bialas et al., 2007). Data from three cores on a transect towards South Tower (GC40, GC41, GC42, Fig. 1) show biogeochemical changes from a situation driven by organic matter degradation to one dominated by anaerobic methane oxidation (AMO) (Fig. 8). This typically results from an increased methane flux from below that consumes the sulphate dissolved in the pore water. Approaching the seep area from the southwest pore water profiles do not exhibit the typical curvature that would indicate significant upward directed fluid flow, but a shape indicating gas bubble-induced pore water irrigation (Haeckel et al., 2007). In addition, the onset of sulphate consumption becomes shallower towards the seep site because of an increasing methane transport from below. Therefore, we can conclude that methane is primarily transported to the sediment surface by gas bubbles rising through the sediment. These bubbles will partly dissolve in the pore water and contribute additionally to the AMO. Furthermore, we can infer from the observed dissolved sulphate gradients that methane hydrate will likely exist at sediment depths below 10–15 m at the sites of GC41 and GC42.

5.2. Heat flow

Thermal gradient data have been collected along CSEM Profile 1 using THP temperature sensors attached to the gravity corer over an

active length of 2 m. All measurements are outside the seeps with the exception of Takahe where thermal gradient data have been collected within a seep (GC43). Outside the seeps the thermal gradients range from 24 to 49 mK/m, which is exactly within the range of BSR inferred regional heat flow of 35–45 mW/m² (Henrys et al., 2003) assuming normal thermal conductivity values between 0.8 and 1.1 W/m/K and minor effects of bottom water temperature variations. A maximum thermal gradient of 119 mK/m (heat flow of 95–130 mW/m²) has been observed inside Takahe as well as veins of gas hydrate and gas filled sediments in the uppermost 2.5 m (Fig. 9). This thermal anomaly may indicate that thermally driven fluid expulsion could play a role (Poort et al., 2007) which would hamper the formation of gas hydrate and explain the low hydrate concentration beneath Takahe.

Fig. 10 shows a sketch of CSEM Profile 1 based on observations described in this paper and in Netzeband et al. (2009-this issue). CSEM reveals a layer of highly porous and conductive sediments close to the seafloor. The main upward fluid and gas transport happens along faults interrupting the BSR and methane may be transported all the way up to or near the seafloor. Below South Tower a gas hydrate reservoir has accumulated at intermediate depths. This gas hydrate sweet spot may also be the source for shallow free gas through hydrate dissociation on top of the GHSZ. Deep carbonate crust formed during past seep activity may also be present. The gas migrates through shallow fissures and cracks to the seafloor where it is released to the seawater producing gas flares as seen in hydro-acoustic data. At South Tower geochemical profiles also indicate increased free methane transport by gas bubbles which can be partly dissolved in the pore water. High amplitude reflections above the BSR have been observed along seismic transects near North Tower. In Fig. 10 we adopted the line-drawing of Seep D at North Tower in Netzeband et al. (2009-this issue, Figs. 4 and 10 therein) and projected that feature onto our conceptual model assuming a similar seep structure could be also present at South Tower. Takahe is characterized by a seismically inferred seep (Seep A, Netzeband et al., 2009-this issue, Figs. 3 and 7

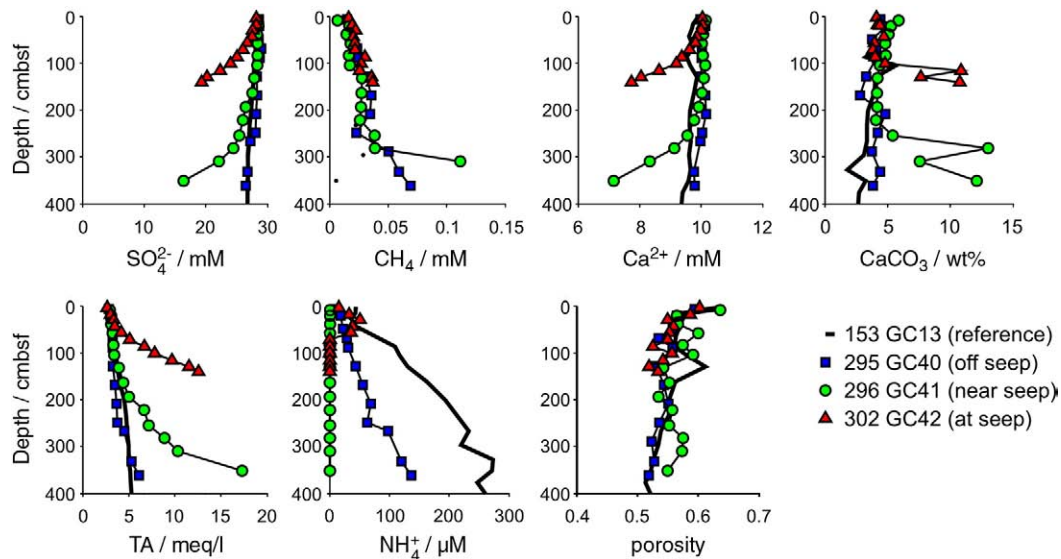


Fig. 8. Geochemical data of gravity cores taken across South Tower along CSEM Profile 1. Towards the seep, the methane flux increases and thus the reaction zones of AMO and the corresponding precipitation of calcium carbonate become shallower (see profiles of SO_4^{2-} , TA, Ca^{2+} , CaCO_3). In the same direction, NH_4^+ concentrations decrease, indicating decreasing importance of organic matter degradation.

therein) which is interpreted as a gas chimney and indicates methane transport from below the BSR. Higher heat flow observed at this site could be a sign that the gas hydrate stability field is disturbed and the formation of gas hydrate is restricted to shallower levels. Gas hydrate has been retrieved from shallow cores and the slightly elevated resistivity values observed in the CSEM data at intermediate depth at this site could be pockets of gas or gas hydrate filled sediments.

6. Conclusions

CSEM data collected on Opouawe Bank in the Wairarapa region with a bottom-towed electric dipole–dipole system provide important information on the gas hydrate distribution within the stability field. Highly anomalous resistivities (10 Ωm and above) have been observed below North Tower and South Tower. Both are active seep sites indicated by flares escaping from the seafloor, widespread carbonate

crusts, and seismically inferred venting. We conclude that considerable amounts of gas hydrate have accumulated at intermediate depth below these seeps. A total gas hydrate volume of $4.46 \times 10^5 \text{ m}^3$ distributed within the first 100 mbsf has been estimated from apparent resistivities at South Tower. Takaha is a smaller seep site where slightly elevated resistivities have been observed. These could be caused by patchy gas hydrate and gas pockets, but sediment heterogeneities and carbonates could also play a role as well as thermally driven upward fluid flow indicated by the observed higher heat flow at this seep site. The observation of several seismically inferred seeps indicates that the fluid flow is accordingly high in the survey area and large amounts of methane are transported upward through the gas hydrate stability zone, particularly along major faults. Geochemical pore water data of three cores towards South Tower also reflect a higher methane flux towards the seep by shallow anaerobic methane oxidation. At South Tower, gas hydrate at intermediate depths may also be the

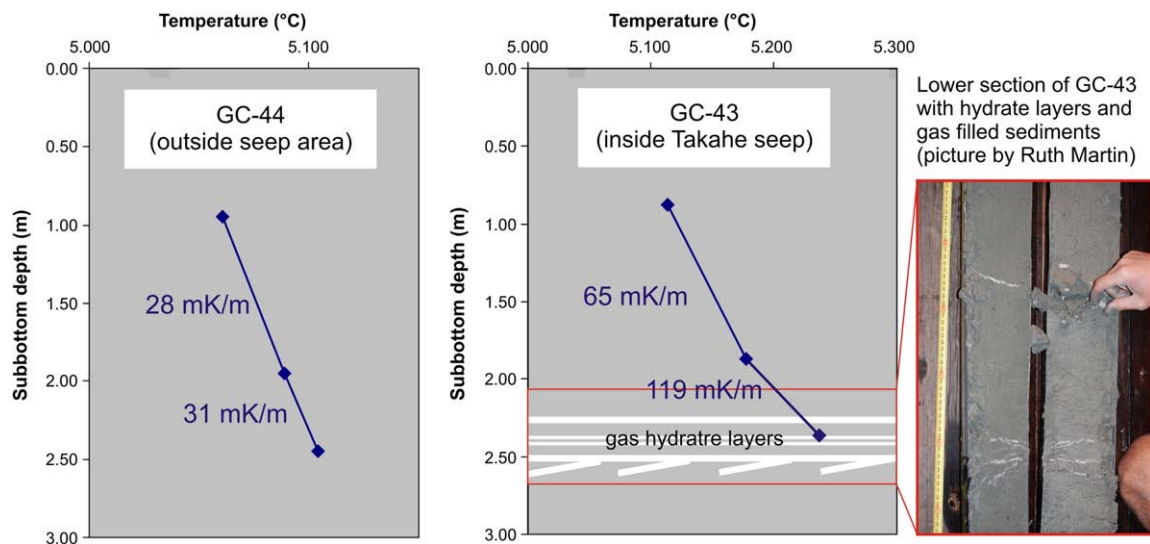


Fig. 9. Example of two temperature depth profiles along Profile 1. GC44 is located outside Takaha and shows a normal, near linear thermal gradient. GC43 was measured inside Takaha and shows a non-linear increase indicating higher heat flow within the seep. GC43 was also the only site along the profile where gas hydrate has been found in thin layers around 2.5 m below seafloor.

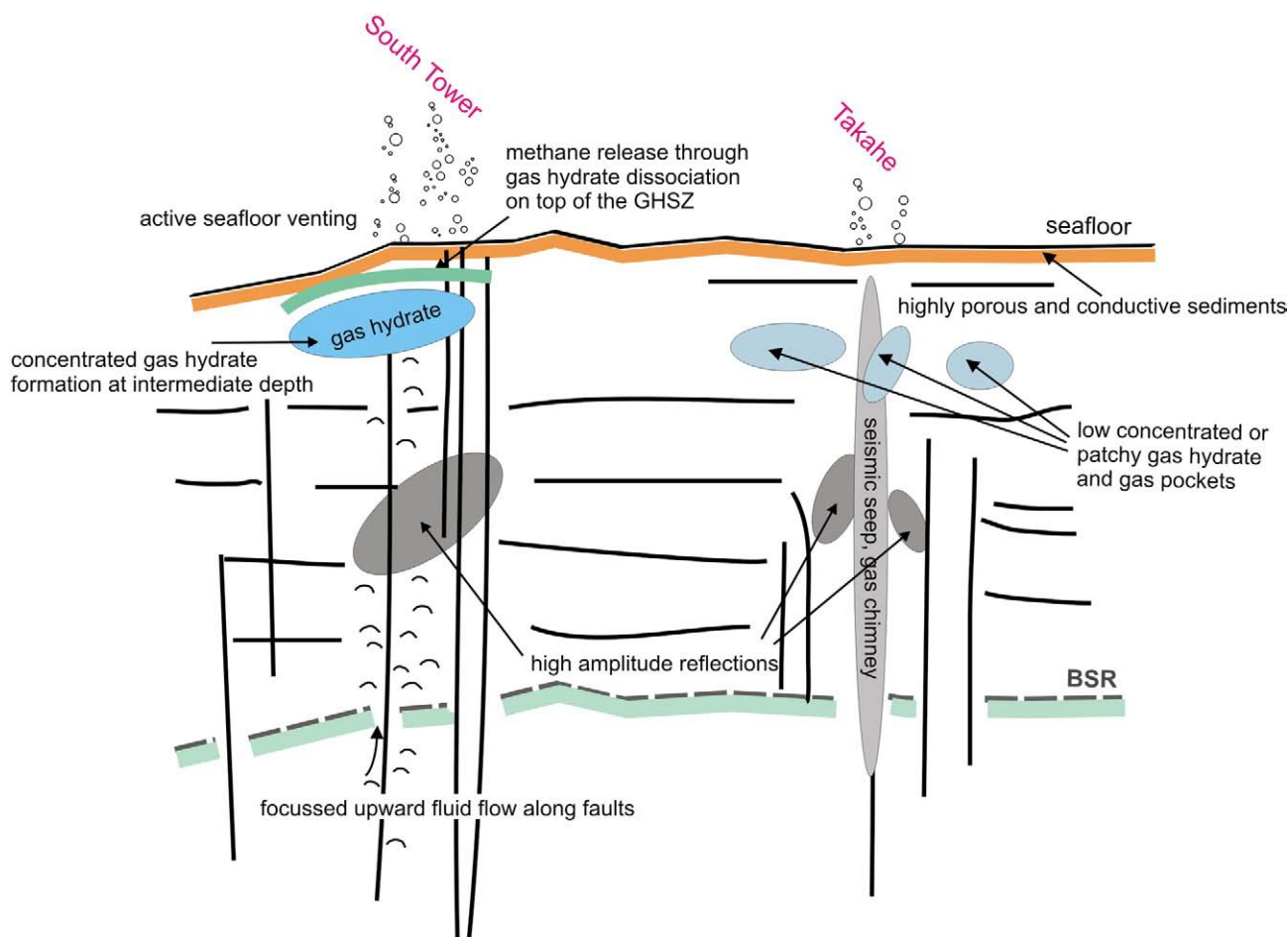


Fig. 10. Conceptual model along Profile 1 based on geophysical and geochemical results. Seismic reflection data reveal a strong BSR indicating the existence of free gas at the base of the gas hydrate stability zone (BGHSZ) that is interrupted by faults which can act as conduits for upward methane and fluid transport. High amplitude reflections occur above the BGHSZ (Netzeband et al., 2009–this issue). At South Tower CSEM data reveal a layer of elevated gas hydrate concentration at intermediate depth. This layer may serve as a reservoir of methane that migrates through cracks and fissures and shallow porous sediments to the seafloor where bubbles and flares indicate active seafloor venting. At Takahe, gas hydrate and gas pockets, both of low concentration, may have accumulated at depth below the seep.

source for shallow free gas through hydrate dissociation on top of the GHSZ.

Acknowledgements

Thanks to the captain and crew of voyage SO191 Leg 1 for support during the experiments. Special thanks to David Keen, GNS, NZ, for technical assistance during the cruise. Thanks to Carsten Scholl for supplying his 1D code and ongoing discussions. We thoroughly thank the editors and two reviewers for their very helpful and detailed comments. The “New Vents” project was funded by the German Ministry of Education and Research BMBF, Grant No. 03G0191A. Jeffrey Poort was also supported by the Flemish Fund for Scientific Research (FWO–Vlaanderen).

References

- Archie, G.E., 1942. The electrical resistivity log as an aid in determining some reservoir characteristics. *J. Pet. Technol.* 5, 1–8.
- Barnes, P.M., Lamarche, G., Bialas, J., Henrys, S., Pecher, I.A., Netzeband, G.L., Greinert, J., Mountjoy, J.J., Pedley, K., Crutchley, G., 2009–this issue. Tectonic and geological framework for gas hydrates and cold seeps on the Hikurangi Subduction Margin, New Zealand. *Mar. Geol.* doi:10.1016/j.margeo.2009.03.012.
- Bialas, J., Greinert, J., Linke, P., Pfannkuche, O., 2007. FS Sonne cruise report SO191, project “New Vents.”. Report from Leibniz Institute of Ocean Science at CAU Kiel, Germany, No.9.
- Cheesman, S.J., Edwards, R.N., Chave, A.D., 1987. On the theory of sea-floor conductivity mapping using transient electromagnetic systems. *Geophysics* 52 (2), 204–217.

- Collett, T., Riedel, M., Cochran, J., Bosweel, R., Presley, J., Kumar, S., Sathe, A., Lall, M., Sibal, V., NGHP Expedition 01 Scientists, 2008. Indian National Gas Hydrate Program, Expedition 01 initial reports. Directorate General of Hydrocarbons, Ministry of Petroleum and Natural Gas, India.
- Davy, B., Wood, R., 1994. Gravity and magnetic modelling of the Hikurangi Plateau. *Mar. Geol.* 118, 153–173.
- Edwards, R.N., 1997. On the resource evaluation of marine gas hydrate deposits using sea-floor transient electric dipole–dipole method. *Geophysics* 62 (1), 63–74.
- Ellis, M., Evans, R.L., Hutchinson, D., Hart, P., Gardner, J., Hagen, R., 2008. Electromagnetic surveying of seafloor mounds in the Gulf of Mexico. *Mar. Pet. Geol.* 25 (9), 960–968.
- Evans, R.L., Law, L.K., Louis, B., Cheesman, S., Sananikone, K., 1999. The shallow porosity structure of the continental shelf of the Eel Shelf, Northern California: results of a towed electromagnetic survey. *Mar. Geol.* 154, 211–226.
- Faure, K., Greinert, J., Pecher, I.A., Graham, I.J., Massoth, G.J., deRonde, C.E., Wright, I.C., Baker, E. T., Olson, E.J., 2006. Methane seepage and its relation to slumping and gas hydrate at the Hikurangi margin, New Zealand. *N.Z. J. Geol. Geophys.* 49, 503–516.
- Greinert, J., Lewis, K.B., Bialas, J., Pecher, I.A., Rowden, A., Linke, P., De Batist, M., Bowden D.A., Suess, E. Methane seepage along the Hikurangi Margin, New Zealand: review of studies in 2006 and 2007. *Marine Geology*, in review.
- Haeckel, M., Wallmann, K., Boudreau, B.P., 2007. Bubble-induced porewater mixing: a 3-D model for deep porewater irrigation. *Geochim. Cosmochim. Acta* 71 (21), 5135–5154.
- Henrys, S., Ellis, S., Uruski, C., 2003. Conductive heat flow variations from bottom simulating reflectors on the Hikurangi margin. *N. Z. Geophys. Res. Lett.* 30 (2), 1065–1068.
- Jackson, P.D., Taylor-Smith, D., Stanford, P.N., 1978. Resistivity–porosity–particle shape relationships for marine sands. *Geophysics* 43, 1250–1268.
- Katz, H.R., 1982. Evidence for gas hydrates beneath the continental slope, East Coast, North Island, New Zealand. *N.Z. J. Geol. Geophys.* 25, 193–199.
- Klaucke, I., Weinrebe, W., Petersen, C.J., Bowden, D., 2009–this issue. Temporal variability of gas seeps offshore New Zealand: multi-frequency geoaoustic imaging of the Wairarapa area, Hikurangi margin. *Mar. Geol.* doi:10.1016/j.margeo.2009.02.009.
- Lewis, K.B., Marshall, B.A., 1996. Seep faunas and other indicators of methane-rich dewatering on New Zealand convergent margins. *N.Z. J. Geol. Geophys.* 39, 181–200.
- Netzeband, G., Krabbenhoft, A., Zillmer, M., Petersen, C.J., Papenberg, C., Bialas, J., 2009–this issue. The structures beneath submarine methane seeps: seismic evidence

- from Opouwe Bank, Hikurangi Margin, New Zealand. *Mar. Geol.* doi:10.1016/j.margeo/2009.07.005.
- Pecher, I.A., Henrys, S.A., Zhu, H., 2004. Seismic images of gas conduits beneath vents and gas hydrates on Ritchie Ridge, Hikurangi margin, New Zealand. *N.Z. J. Geol. Geophys.* 47, 275–279.
- Poort, J., Kutas, R.I., Klerkx, J., Beaubien, S.E., Lombardi, S., Dimitrov, L., Vassilev, A., Naudt, L., 2007. Strong heat flow variability in an active shallow gas environment, Paleo-Dnepr, Black Sea. *Geo Mar. Lett.* 27, 185–195. doi:10.1007/s00367-007-0072-4.
- Riedel, M., Spence, G.D., Chapman, N.R., Hyndman, R.D., 2002. Seismic investigations of a vent field associated with gas hydrates, offshore Vancouver Island. *J. Geophys. Res.* 107 (B9). doi:10.1029/2001JB000269.
- Riedel, M., Collett, T.S., Malone, M.J., and the Expedition 311 Scientists, 2006. Cascadia Margin Gas Hydrates. In: *Proceedings of the Integrated Ocean Drilling Program*, vol. 311. IODP Management International Inc. doi:10.2204/iodp.proc.311.102.2006.
- Schwalenberg, K., Willoughby, E.C., Mir, R., Edwards, R.N., 2005. Marine gas hydrate electromagnetic signatures in Cascadia and their correlation with seismic blank zones. *First Break* 23, 57–63.
- Schwalenberg, K., Wood, W.T., Pecher, I.A., Hamdan, L.J., Henrys, S.A., Jegen, M.D., Coffin, R.B. Preliminary interpretation of electromagnetic, heat flow, seismic, and geochemical data for gas hydrate distribution across the Porangahau Ridge, New Zealand. *Marine Geology*, in review.
- Townend, J., 1997. Estimates of conductive heatflow through bottom simulating reflectors on the Hikurangi and southwest Fjordland continental margins. *N. Z. Mar. Geol.* 141, 209–220.
- Weitemeyer, K.A., Constable, S.C., Key, K.W., Behrens, J.P., 2006. First results from a marine controlled-source electromagnetic survey to detect gas hydrates offshore Oregon. *Geophys. Res. Lett.* 33. doi:10.1029/2005GL024896.
- Yuan, J., Edwards, R.N., 2000. The assessment of marine gas hydrates through electrical remote sounding: hydrate without a BSR? *Geophys. Res. Lett.* 27, 2397–2400.